ISSN: 0256-307X

中国物理快报
Chinese Physics Letters

Volume 32 Number 6 June 2015

A Series Journal of the Chinese Physical Society
Distributed by IOP Publishing

Online: http://iopscience.iop.org/0256-307X
http://cpl.iphy.ac.cn

CHINESE PHYSICAL SOCIETY
IOP Publishing

CHIN. PHYS. LETT. Vol. 32, No. 6 (2015) 064302

The Effects of Seamounts on Sound Propagation in Deep Water *

LI Wen(李文)[1,3], LI Zheng-Lin(李整林)[1,2**], ZHANG Ren-He(张仁和)[1], QIN Ji-Xing(秦继兴)[1], LI Jun(李鋆)[1,3], NAN Ming-Xing(南明星)[4]

[1] *State Key Laboratory of Acoustics, Institute of Acoustics, Chinese Academy of Sciences, Beijing 100190*
[2] *Haikou Laboratory of Acoustics, Institute of Acoustics, Chinese Academy of Sciences, Haikou 570105*
[3] *University of Chinese Academy of Sciences, Beijing 100190*
[4] *General Staff MET-HYD Department, Beijing 100081*

(Received 2 March 2015)

A propagation experiment was conducted in the South China Sea in 2014 with a flat bottom and seamounts respectively by using explosive sources. The effects of seamounts on sound propagation are analyzed by using the broadband signals. It is observed that the transmission loss (TL) decreases up to 7 dB for the signals in the first shadow zone due to the seamount reflection. Moreover, the TL might increase more than 30 dB in the converge zone due to the shadowing by seamounts. Abnormal TLs and pulse arrival structures at different ranges are explained by using the ray and wave theory. The experimental TLs and arrival pulses are compared with the numerical results and found to be in good agreement.

PACS: 43.30.Cq, 43.30.Dr, 92.10.Vz DOI: 10.1088/0256-307X/32/6/064302

Seamounts in deep water have significant effects on sound propagation. Over the past several decades, physical experiments and theoretical approaches have been explored. However, the phenomena of acoustic propagation around seamounts are not well understood due to the complexities and uncertainties from oceanographic variability and the geo-acoustic property of the sea bottom.[1−3]

A series of sound propagation experiments over the seamounts have been conducted. One of the first experiments was carried out in 1968,[4,5] in which explosive signals were dropped in the northeast Pacific as the sources and hydrophones located near Midway and Wake islands to record signals, respectively. The experiment showed that the peak pressure levels recorded at Wake were as much as 35 dB below those at Midway and the spectral energy density ratio between Wake and Midway was frequently independent. Another experiment was carried out over the Dickins Seamount in the northeast Pacific ocean in 1975[6,7] by using both explosive shots and CW sources. The results showed that the increased TL was up to 15 dB for the shallow source in which all deep refracted waves could be blocked by the seamount and the shadowing loss behind the seamount was an $f^{1/2}$ dependence at frequencies larger than 50 Hz.

Kim investigated the physical characteristics of sound propagation around seamounts.[1] The broadband pulses measured from the BASSEX experiment carried in the northeast Pacific around the Kermit–Roosevelt seamounts in 2004. It was found that the shadow and convergence zones behind the seamounts were matched well between the experimental data and the 2D and 3D sound propagation models. However, reconciliation of the broadband pulses behind the seamount was more challenging due to the complicated environment. It is worth experimentally investigating the effects of seamounts on sound propagation in deep water further.

In this Letter, a sound propagation experiment with the presence of seamounts conducted in the South China Sea is introduced firstly. The TLs along two propagation tracks with and without seamounts are compared. The numerical TLs are simulated to compare with the experimental data. Furthermore, the arrival pluses and ray diagram are analyzed to show the effects and mechanisms of seamounts on sound propagation in deep water.

In 2014, an experiment of sound propagation was conducted in the deep water area of the South China Sea. The receiving array made by 24 distributed underwater signal recorders (USR) from 130 m to 1800 m with different intervals was moored at the bottom. The sample rate of hydrophones is 8000 Hz. The wide band signals (WBS) charged with 1 kg TNT were dropped from Chinese *R/V* Shi Yan 1 from the Institute of Acoustics, Chinese Academy of Sciences along two propagation tracks with and without seamounts. The nominal detonation depth of WBS is 200 m.

The bathymetries along the propagation tracks with and without seamounts are given in Fig. 1. The top of the first seamount is 800 m below sea surface and in a 30 km range from the receiving array. The bottom along the propagation track without seamounts is relatively flat, which is called flat bottom, and the average depth is about 4305 m. The

*Supported by the National Nature Science Foundation of China under Grant Nos 11434012 and 11174312.
**Corresponding author. Email: lzhl@mail.ioa.ac.cn

sound speed profile shown in Fig. 2 was measured by XBT in the experiment. The depth of the sound channel axis is about 1200 m and the sound speed at the bottom is 1532 m/s, which is less than that at sea surface, 1544 m/s.

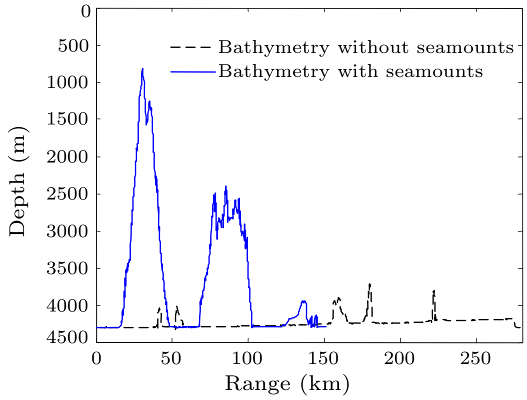

Fig. 1. Bathymetry along two propagation tracks.

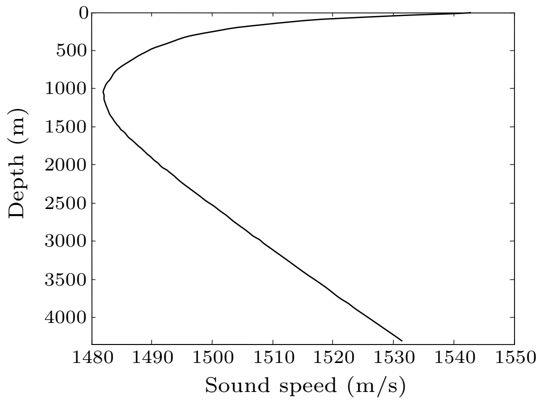

Fig. 2. Sound speed profile measured in the experiment.

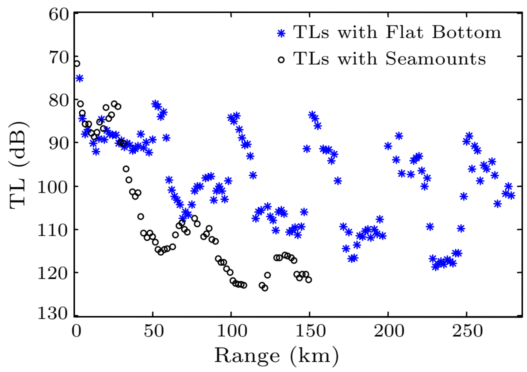

Fig. 3. TLs along two tracks with/without seamounts, for a central frequency of 300 Hz, a source depth of 200 m, and a receiver depth of 170 m.

The measured spectra are averaged in the 1/3-octave bandwidth. The narrow band energy of the propagation signal is represented as

$$E(f_0) = \frac{2}{F_s^2}\frac{1}{nf_2 - nf_1 + 1}\sum\nolimits_{i=nf_1}^{nf_2}|X_i|^2, \quad (1)$$

where X_i represents the FFT spectrum of the signal $x(t)$ at the ith frequency bin, f_0 is the central frequency, F_s is the sample rate, and nf_1 and nf_2 are the start and end frequency numbers for the frequency band, respectively.

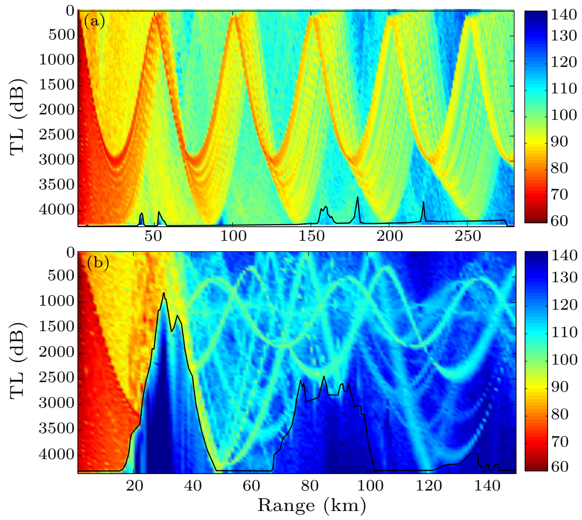

Fig. 4. TLs for environments without seamounts (a) and with the presence of seamounts (b), for a central frequency of 300 Hz, and the source depth of 200 m.

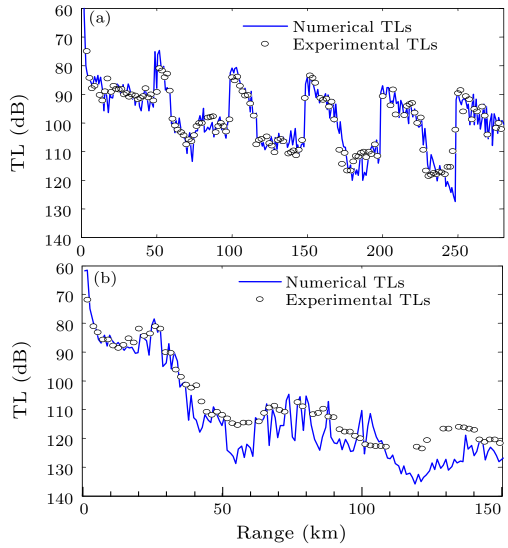

Fig. 5. Comparison of the numerical TLs and experimental TLs for environments without seamounts (a) and with the presence of seamounts (b), for a central frequency of 300 Hz, a source depth of 200 m, and a receiver depth of 170 m.

The TL can be denoted as

$$TL(f_0) = S(f_0) - (10\log(E(f_0)) - b), \quad (2)$$

where S is the source level, and b is the sensitivity of the hydrophones.

TLs are shown in Fig. 3 for the conditions with and without seamounts, where the central frequency is 300 Hz, and the receiver depth is 170 m. It can be seen from Fig. 3 that the TLs for the environment with the seamounts decrease down to 7 dB in the range of

28 km and increase more than 30 dB in the range of 56–62 km compared with those for the environment without the seamounts.

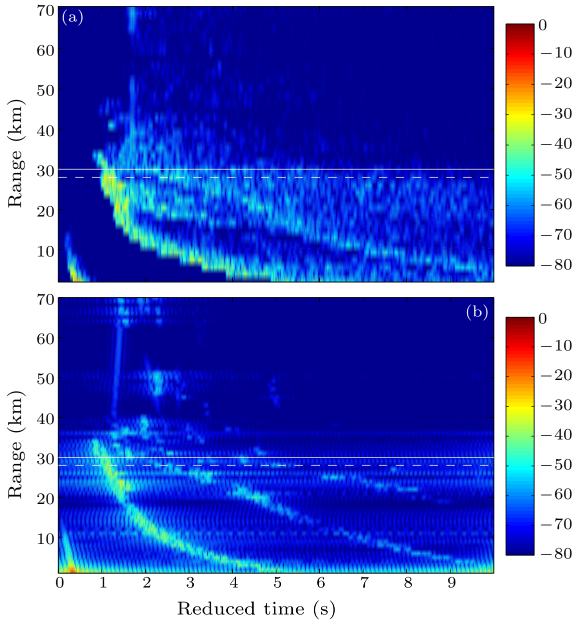

Fig. 6. The 2D color map of range-stacked arrival pulses, (a) experimental results and (b) numerical results, for a source depth of 200 m, a receiver depth of 170 m, a central frequency of 300 Hz and a bandwidth of 10 Hz.

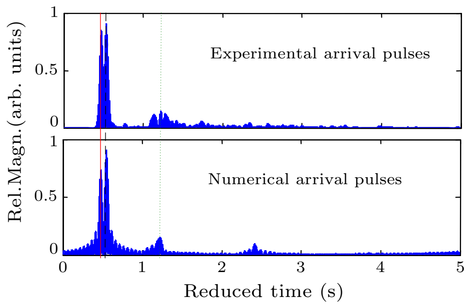

Fig. 7. Comparison of numerical arrival pulses with the experimental results in the range of 28 km indicated by horizontal dashed lines in Fig. 6.

To explain the results shown in Fig. 3, the BELLHOP ray model[8] is used to calculate the propagation sound field for the environments with/without seamount. According to the principle of reciprocity,[7] the positions of source and receiver are exchanged in the calculation. The bottom parameters were measured through core sampling in the experiment. Sample analysis results show that the bottom type is silty clay. For the sake of great dispersion of sound speed in the sediment, preliminary inversion[9] was implemented. Then, a two-layer fluid bottom model is established with a sediment thickness of 5 m, a sediment sound speed of 1565 m/s, a sediment density of 1.6 g/cm^3, a sediment attenuation coefficient of 0.09 dB/m, a basement sound speed of 1650 m/s, a basement density of 1.8 g/cm^3 and a basement attenuation coefficient of $0.4 \times (f/1000)^{0.9}$ dB/λ,[9] where f is in units of kHz.

Figure 4 shows the two-dimensional TL for the environments with and without seamounts, in which the source depth is 200 m, and the central frequency is 300 Hz. It can be seen from Fig. 4 that ranges of 28 km and 56–62 km in Fig. 3 represent the first shadow zone and the first convergence zone for the flat bottom environment, respectively. Comparing Figs. 4(a) and 4(b), we find that sound signals can be reflected to the receivers in the shadow zone from the up sloping bottom of the first seamount. It causes the intensities near the range of 28 km for the seamount environment to be higher than that of the flat bottom environment. For the range greater than the site of the first seamount, the sound energy is shadowed by the seamounts. Therefore, the convergence structures of the sound field in deep water are destroyed, and TLs increase more than 30 dB. A comparison of the numerical TLs and experimental TLs along two different tracks is shown in Fig. 5 for the receiver depth at 170 m. It can be seen that the numerical TLs are in good agreement with the experimental TLs. Although the problems with seamounts are complex, the TLs can still predicted very well, and the effects of the seamounts on sound propagation are obvious. The small differences between numerical TLs and experimental TL for the range larger than 50 km may be caused by the errors of geo-acoustic properties and the slope bathymetry.

Next, arrival structure of pulse signals are analyzed for the seamount environment. The numerical and experimental range-stacked arrival pulses[6] are given in Figs. 6 and 7, where the central frequency is 300 Hz with a bandwidth of 10 Hz. Figure 7 gives the results in the range of 28 km. The reduced time of the horizontal coordinate in Figs. 6 and 7 is computed by subtracting the propagation time from the arrival time. The color values in Figs. 6 and 7 are denoted as

$$E = 20 \log_{10}(p(r,t)/p_{\max}(r,t)), \tag{3}$$

where p is the sound pressure, and $p_{\max}$ is the maximum of p. The value of the vertical coordinate in Fig. 7 is the normalized amplitude. The white solid lines in Fig. 6 are at the positions of the top of the first seamount. There is a maximal intensity at 28 km for both simulation and experiment results because more rays can arrive in this range. The ray diagram is displayed in Fig. 8. There are three main kinds of rays denoted by three kinds of colored lines. Combining Figs. 7 and 8, the first arrival pulse marked by the solid red line undergoes one bottom reflection (1BR), the second arrival pulse marked by the dashed dark line undergoes 1BR and one surface reflection (1SR) or 2SR, and the third pulse marked by the dotted green line undergoes 2BR and 1SR. The amount of rays that undergo 1BR for the environment with the seamount is twice of the rays in the flat bottom environment. Moreover, the rays marked with the same color and undergoing the same reflections in Fig. 8 have approximate amplitude and phase. Additionally, other rays which undergo more than 1BR can also reach the receiver. Here $20\log_{10} 2$ approximately equal to 6 dB. Therefore, the TLs around 28 km decrease up to 7 dB. In the shadow zone (52–62 km) of the seamount, the numerical arrival pulse can roughly match with the experimental results. In fact, the geo-acoustic properties and slope bathymetry of the first seamount play important roles in the reflection. Small errors for these parameters in the model can cause the differences. This is a challenging problem and may be related to ray chaos.[6]

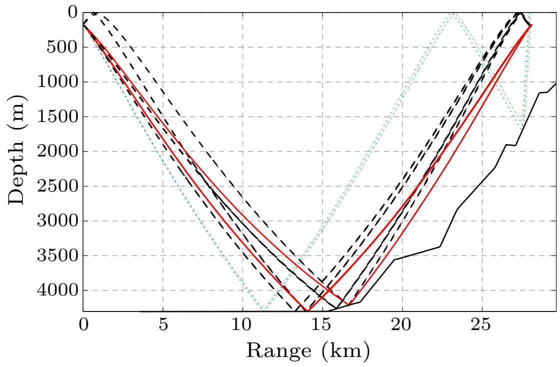

Fig. 8. Eigen rays from the source to the receiver in the range of 28 km, for a source depth of 200 m and a receiver depth of 170 m.

In summary, an experiment has been carried out to investigate the effects of seamounts on sound propagation in deep water. Obvious TL differences for propagation in the environments with and without seamounts are observed. Under conditions where the seamount is located in the first shadow zone, the TLs decrease up to 7 dB for the ranges before the top of the seamount due to the reflection of bathymetry. The convergence zone structure appearing in the deep water with a flat bottom environment might be destroyed by the direct blockage of the seamount and TLs increase more than 30 dB after passing the seamount. Abnormal TLs and pulse arrival structures in different ranges are explained by using the ray theory. The numerical TLs and pulse arrival structures can match with the experimental results very well. Next, a statistical approach will be used to explain some sound propagation phenomena after the seamounts.

We thank all the staff for participating in the experiment and developing the sources and receivers.

References

[1] Kim H J 2009 *PhD Dissertation* (Boston: Massachusetts Institute of Technology)
[2] Peng Z H and Zhang R H 2005 *Acta Acust.* **30** 97 (in Chinese)
[3] Zhang R H, He Y, Liu H and Akulichev V A 1995 *J. Sound Vib.* **184** 43
[4] Northrop J 1970 *J. Acoust. Soc. Am.* **48** 417
[5] Nutile D A and Guthrie A N 1979 *J. Acoust. Soc. Am.* **66** 1813
[6] Champan N R and Ebbeson G R 1983 *J. Acoust. Soc. Am.* **73** 1979
[7] Ebbeson G R and Turner R G 1983 *J. Acoust. Soc. Am.* **73** 143
[8] Jensen F B, Kuperman W A, Porter M B and Schmidt H 2011 *Comput. Ocean Acoustic* 2nd edn (New York: Springer) chap 3 p 155
[9] Li Z L and Zhang R H 2004 *Chin. Phys. Lett.* **21** 1100
[10] Qin J X et al 2014 *Sci. Chin. Phys. Mech. Astron.* **57** 1031

Chinese Physics Letters

Volume 32 Number 6 June 2015

CONDENSED MATTER: ELECTRONIC STRUCTURE, ELECTRICAL, MAGNETIC, AND OPTICAL PROPERTIES

CROSS-DISCIPLINARY PHYSICS AND RELATED AREAS OF SCIENCE AND TECHNOLOGY

ERRATA AND OTHER CORRECTIONS